Journal of the Optical Society of America B
OPTICAL PHYSICS

Extreme robustness of Jackiw–Rebbi states in binary waveguide arrays under strong disturbance

TRUONG X. TRAN

Department of Physics, Le Quy Don Technical University, 236 Hoang Quoc Viet str., 100000 Hanoi, Vietnam (tranxtr@gmail.com)

Received 6 June 2019; revised 18 July 2019; accepted 29 July 2019; posted 30 July 2019 (Doc. ID 369435); published 22 August 2019

We investigate the robustness of quantum relativistic Jackiw–Rebbi states, which have been found recently in a system consisting of two interfaced binary waveguide arrays with opposite propagation mismatches. For comparison, we study the robustness under strong disturbance during propagation of Jackiw–Rebbi states and quantum relativistic Dirac solitons, which have also been found earlier in binary waveguide arrays. We prove that these Jackiw–Rebbi states are extremely robust even under strong disturbance, as opposed to Dirac solitons.

https://doi.org/10.1364/JOSAB.36.002559

1. INTRODUCTION

Various fundamental photonic phenomena such as discrete diffraction [1,2], discrete solitons [1,3–5], diffractive resonant radiation [6], and supercontinuum generation in both frequency and wavenumber domains [7,8] have been found in waveguide arrays (WAs). These platforms have also attracted a great amount of interest in mimicking fundamental effects in nonrelativistic quantum mechanics such as Bloch oscillations [1,9–11] and Zener tunneling [12]. However, in order to investigate relativistic quantum mechanics phenomena arising from the Dirac equations, one has to use binary WAs (BWAs) instead of conventional WAs. Recently, many important relativistic quantum mechanics phenomena, such as *Zitterbewegung* [13], Klein paradox [14], and Dirac solitons (DSs) in the nonlinear regime [15], have been found in BWAs.

The discrete gap solitons in BWAs in the classical context have been explored much earlier [16–21]. However, only recently, these discrete solitons in BWAs have been shown to be optical analogs of DSs in a one-dimensional (1D) nonlinear relativistic quantum Dirac equation [15]. The stability dynamics of DSs and interaction between them have been investigated in [22]. The generation and dynamics of two-dimensional DSs in square binary waveguide lattices have been investigated in [23]. The higher-order DSs in BWAs and its properties have been studied in [24]. The Dirac light bullet, which maintains its profile in both space and time domains, has been shown to exist in BWAs in [25]. The switching effect of a DS by an extremely weak signal in BWAs with varying propagation mismatch has been investigated in [26], where the compression, symmetry conservation, and symmetry breaking of DSs have also been analyzed in details. It is worth mentioning that nonlinear Dirac equations have been studied for a long time. The first nonlinear model of the Dirac equation was initially introduced by Ivanenko in 1938 for self-interacting electrons [27]. Heisenberg also used the nonlinear Dirac equation in an attempt to formulate a unified theory of elementary particles in 1957 [28]. In 1970, Soler re-introduced Ivanenko's model in the context of extended nucleons [29,30].

Recently, it has been proved in [31] that one can create the optical analog of special states, known in the quantum field theory as *Jackiw–Rebbi* (JR) solutions [32] at the interface of two BWAs, which are described by two Dirac equations with so-called Dirac masses of different signs. The analytical solutions for JR states in BWAs have been found in [31] in the linear regime. Meanwhile, the solutions for JR states in BWAs with Kerr nonlinearity have been investigated quite recently in [33]. The interaction between JR states and DSs in BWAs has been investigated in [34]. Based on the JR states, the charge fractionalization phenomenon, which plays a central role in the fractional quantum Hall effect [35], has been predicted. One of the spectacular properties of the JR states is the topological nature of its zero-energy solution, which can be considered as a precursor to topological insulators [36]. It has been demonstrated that topological photonics can have a great potential in the development of robust optical circuits [37].

In this work, we study the stability and robustness of JR states in BWAs under very strong disturbance. For comparison, we investigate the dynamics of JR states and DSs under strong disturbance of different types and show that the JR states are extremely robust as compared to DSs in the same conditions.

The paper is organized as follows. In Section 2, as a starting point, we show the pure JR states and DSs, i.e., without any disturbance in BWAs. Then, in Section 3, we investigate the robustness of JR states and DSs when the nonlinearity is turned on/off. In Section 4, we explore the robustness of JR states and

DSs when the system is under transverse linear potential. In Section 5, we study the robustness of JR states and DSs when these structures are launched obliquely into the system at the input. Finally, in Section 6, we summarize our results and finish with concluding remarks.

2. JACKIW–REBBI STATES AND DIRAC SOLITONS WITHOUT DISTURBANCE

In this section, as a starting point, we show the dynamics of pure JR states and DSs, i.e., when they propagate in an ideal condition without any disturbance. These results have already been obtained earlier for DSs in [15] and quite recently for JR states in [31].

Light propagation in BWAs with Kerr nonlinearity can be described, in the continuous-wave regime, by the following dimensionless coupled-mode equations (CMEs) [15,31,34]:

$$i\frac{da_n(z)}{dz}+\kappa[a_{n+1}(z)+a_{n-1}(z)]-(-1)^n\sigma a_n+\gamma|a_n|^2a_n(z)=0, \tag{1}$$

where a_n is the electric field amplitude in the nth waveguide, z is the longitudinal spatial coordinate, 2σ and κ are the propagation mismatch and the coupling coefficient between two adjacent waveguides of the array, respectively, and γ is the nonlinear coefficient of waveguides, which is positive for self-focusing but negative for self-defocusing media.

After setting $\Psi_1(n)=(-1)^n a_{2n}$ and $\Psi_2(n)=i(-1)^n a_{2n-1}$ and following the standard approach [13], we can introduce the continuous transverse coordinate $\xi\leftrightarrow n$ and the two-component spinor $\Psi(\xi,z)=(\Psi_1,\Psi_2)^T$, which satisfies the 1D nonlinear Dirac equation [15]:

$$i\partial_z\Psi=-i\kappa\hat{\sigma}_x\partial_\xi\Psi+\sigma\hat{\sigma}_z\Psi-\gamma G, \tag{2}$$

where the nonlinear terms $G\equiv(|\Psi_1|^2\Psi_1,|\Psi_2|^2\Psi_2)^T$; $\hat{\sigma}_x$ and $\hat{\sigma}_z$ are the usual Pauli matrices. In quantum field theory, the parameter σ in the Dirac equation is often called the mass of the Dirac field (or Dirac mass), and this mass parameter can be both positive and negative.

In order to create JR states, one needs to have at least one interface between two BWAs with opposite propagation mismatches. For waveguides with $n<0$, we have $\sigma=\sigma_1$, whereas for $n\geq 0$, we have $\sigma=\sigma_2$. Note that the condition $\sigma_1\sigma_2<0$ must be held true. The illustrative sketch of this system is depicted in Fig. 1(a) in [31]. At the interface between two adjacent BWAs, the exact analytical localized solutions for JR states have been obtained in [31] in the linear case. In the nonlinear case, as shown in one of our latest works, which will be published elsewhere [33], the JR states can be obtained via the so-called shooting method, which can be implemented by introducing a detuning parameter for the stationary solutions. In this way, one can reduce Eq. (1) into a system of nonlinear algebraic equations, which can be solved by using the shooting method to "shoot" from the soliton center to its vanishing tails. This method has also been successfully used to numerically get the profiles for dissipative Bragg solitons in active nonlinear fibers [38]. In Fig. 1(a), we show the propagation of a JR state of the first type in the ideal condition, i.e., without any disturbance (see also Fig. 1 in [31] for more details). In Fig. 1(c), we plot the profile of this JR state, which is very stable during propagation, as clearly demonstrated in Fig. 1(a). Note that the peak amplitude of JR states is localized at the interface with waveguide positions $n=(-1;0)$.

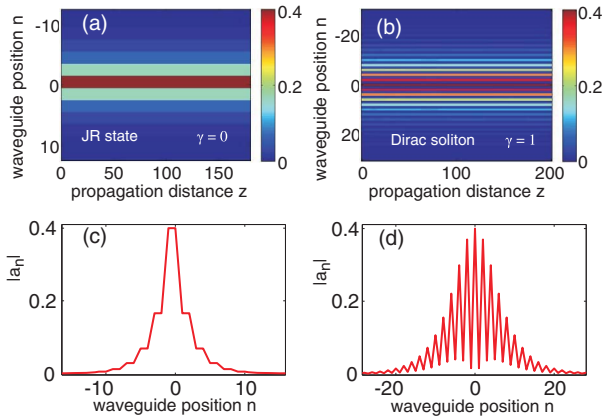

Fig. 1. (a), (b) Propagation of a JR state of the first type and a DS in BWAs, respectively, without any disturbance. (c), (d) Profiles of the JR state and the DS, respectively. Parameters for (a) and (c): coupling coefficient $\kappa=1$, nonlinear coefficient $\gamma=0$, propagation mismatch for the BWA with negative waveguide positions (i.e., $n<0$) $\sigma_1=-1$, propagation mismatch for the BWA with positive waveguide positions (i.e., $n\geq 0$) $\sigma_2=1$, linear potential parameter $\alpha=0$. Parameters for (b) and (d): coupling coefficient $\kappa=1$, nonlinear coefficient $\gamma=1$, propagation mismatch for the whole BWA $\sigma=-1$, linear potential parameter $\alpha=0$.

Meanwhile, in order to create DSs, one just needs a BWA. The analytical solutions for DSs have been obtained in [15]. In Fig. 1(b), we show the propagation of a DS in the ideal condition, i.e., without any disturbance (see also Fig. 2 in [15] for more details). In Fig. 1(d), we plot the profile of this DS, which is also very stable during propagation, as clearly demonstrated in Fig. 1(b). Note that a DS consists of intense and weak components that are localized adjacent to each other. For instance, the intense component is localized at the even waveguides, whereas the weak component is localized at the odd waveguides.

So, in Fig. 1, we have just shown the pure JR state and DS in the ideal condition. In the following sections, we will impose strong disturbance upon these two structures with the aim to investigate their robustness. To estimate real physical parameters of the calculated DSs below, we use typical parameters in WAs made of AlGaAs [39], where the coupling coefficient and nonlinear coefficient in physical units are $K=1240\ \mathrm{m}^{-1}$ and $\Gamma=6.5\ \mathrm{m}^{-1}\ \mathrm{W}^{-1}$, respectively. In this case, the power scale will be $P_0=K/\Gamma=190.8$ W, thus the peak power of the DS and JR state shown in Fig. 1 will be around 30 W, and the length scale in the propagation direction will be $z_0=1/K=0.8$ mm. Indeed, from the dimensionless Eq. (1), one can straightforwardly get back to the system of CMEs in real physical units,

$$i\frac{dA_n}{dZ}+\frac{\kappa}{z_0}[A_{n+1}+A_{n-1}]-(-1)^n\frac{\sigma}{z_0}A_n+\frac{\gamma}{P_0z_0}|A_n|^2A_n=0, \tag{3}$$

by using the following transformations: $a_n = A_n/\sqrt{P_0}$ and $z = Z/z_0$, where the square of the electric field $|A_n|^2$ is in units of the optical power (like the power scale P_0), as is often adopted in fiber optics [5]. So, now it is clear that if we want to set both the dimensionless coupling coefficient κ and the nonlinear coefficient γ equal to unity, as in this work, then we have to choose the length scale $z_0 = \kappa/K = 1/K$ and the power scale $P_0 = \gamma/(\Gamma z_0) = \gamma K/\Gamma = K/\Gamma$, respectively.

3. JACKIW–REBBI STATES AND DIRAC SOLITONS DYNAMICS WHEN THE NONLINEARITY IS TURNED ON/OFF

As mentioned above, in Figs. 1(a) and 1(c), we set $\gamma = 0$ for JR states, whereas in Figs. 1(b) and 1(d), we set $\gamma = 1$ for DSs. The reason for using these specific values of γ is simple: the exact analytical solutions for JR states and DSs are obtained only in the linear and nonlinear regimes, respectively. In this section, we will turn on/off the nonlinearity, i.e., switch on/off the nonlinear coefficient γ in Eq. (1), to see how the pure JR state and DS evolve under this circumstance. In Fig. 2(a), we show the evolution of the JR state in the nonlinear regime (now $\gamma = 1$) when the initial profile is one of the linear JR states plotted in Fig. 1(c). In Fig. 2(c), we plot the input (red curve with round markers) and output (black curve) of this JR state shown in Fig. 2(a). As clearly seen in Figs. 2(a) and 2(c), when the nonlinearity is turned on/off (i.e., γ is switched between 0 and 1), the JR profile is just slightly adjusted at the beginning and quickly becomes perfectly stabilized during propagation. Note again that the profiles of localized nonlinear JR states can be exactly calculated by using some numerical methods, e.g., the shooting method, as shown in [33].

In contrast, one gets totally different scenarios for DSs when the nonlinearity is turned on/off. Indeed, in Fig. 2(b), we show the evolution of the DS in the linear regime (now $\gamma = 0$) when the initial profile is the one of the nonlinear DSs plotted in Fig. 1(d). In Fig. 2(d), we plot the input (red curve) and output (black curve) of this DS shown in Fig. 2(b). It is clearly demonstrated that, unlike JR states, DSs are very sensitive to the switching of the nonlinear coefficient γ. In the nonlinear regime, as shown in Figs. 1(b) and 1(d), one can get a very stable DS due to the well-known balance between the diffraction-based spreading and nonlinearity-based focusing. However, in the linear regime, this balance is broken; as a result, the DS is totally destroyed after a short distance, and we can see a strong spreading of the beam in Figs. 2(b) and 2(d). This linear spreading is also common for all solitons in continuous media, including the well-known solitons obtained from the nonlinear Schrödinger equations in optical fibers [4], if the nonlinearity is switched off.

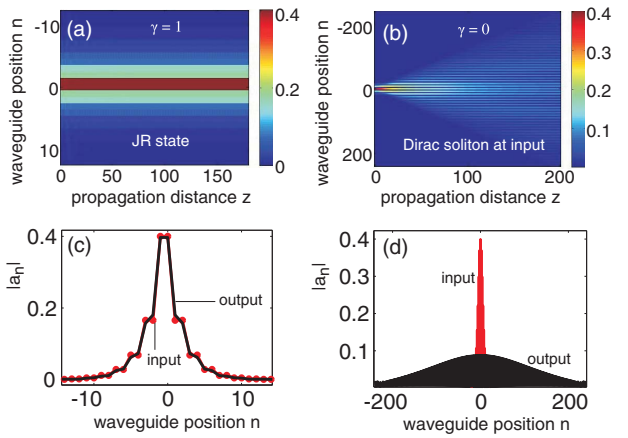

Fig. 2. (a) Propagation of the JR state of the first type shown in Fig. 1(a), but now in the nonlinear regime, i.e., $\gamma = 1$. (b) Propagation of the initial DS shown in Fig. 1(b), but now in the linear regime, i.e., $\gamma = 0$. (c) Input and output profiles of the JR state in (a). (d) Input and output profiles of the beam in (b). All other parameters (except for the nonlinear coefficient γ) are exactly the same as in Fig. 1.

So, we have demonstrated that the JR states are extremely robust if the nonlinearity is turned on/off. This unique feature of JR states is remarkable, because other solitons can be easily destroyed in this circumstance. The reason for this robustness is based on the topological nature of JR states [31], which, as discussed in the Introduction, can have a great potential in the development of robust optical circuits [37].

4. JACKIW–REBBI STATES AND DIRAC SOLITONS DYNAMICS UNDER THE LINEAR POTENTIAL

In this section, we investigate the robustness of JR states and DSs by applying the external transverse linear potential across the system, which changes the propagation constant along the array in a linear fashion. This method has been successfully exploited to generate the photonic analogue of the quantum nonrelativistic Bloch oscillations in WAs [7] by using, for instance, the electro-optic [9] or thermal-optic effect [10]. Mathematically, this linear potential results in adding an extra term $\alpha n a_n$ to the left-hand side of Eq. (1), where the coefficient α is the linear potential parameter. It is well-known that in WAs consisting of identical waveguides, in the linear regime, the linear potential will lead to the Bloch oscillations of beams during propagation in a sinusoidal fashion with a period $z_0 = 2\pi/\alpha$ (see, for instance, Figs. 2(a) and 2(b) in [7] for more details). However, if the nonlinearity is included, then in Was, one can observe the diffractive resonant radiation and the anomalous compensation of the soliton self-wavenumber shift (see Figs. 2(c) and 2(d) in [7] for more details).

As mentioned above, the influence of the linear potential on beam dynamics in WAs has been well-investigated. However, in BWAs, to the best of our knowledge, this influence has not been analyzed so far. Now, we want to investigate the dynamics of initial JR states and DSs in BWAs under the influence of this linear potential. In Fig. 3(a), we show the evolution of the JR state in the linear regime ($\gamma = 0$) with the linear potential parameter $\alpha = 0.02$. The initial profile of the JR state in Fig. 3(a) is the one of the linear JR state plotted in Fig. 1(c). The input (red curve with round markers) and output (black curve) of this JR state are plotted in Fig. 3(c). Note that all other parameters (except for α) are exactly the same as in Fig. 1(a). As clearly demonstrated in Figs. 3(a) and 3(c), the JR state is quite robust under the influence of the linear potential, and its profile is slightly varied during propagation. It is

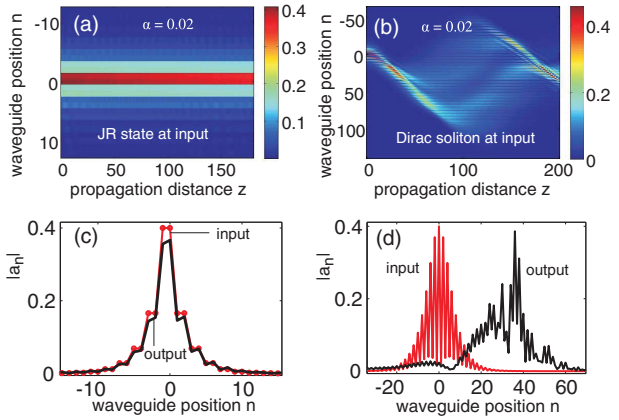

Fig. 3. (a), (b) Propagation of an initial JR state of the first type and an initial DS in BWAs, respectively, when the linear potential parameter $\alpha = 0.02$. (c) Input and output profiles of the JR state in (a). (d) Input and output profiles of the beam in (b). All other parameters (except for α) are exactly the same as in Fig. 1.

worth mentioning that if we use the nonlinear JR states calculated in [33] as the input condition for obtaining Figs. 3(a) and 3(c), then the main above-mentioned features of JR states will remain: the nonlinear JR states are also quite robust with respect to the linear transverse potential, and their profiles are also only slightly changed during propagation.

In contrast, like in the case when the nonlinearity is turned on/off as shown in Fig. 2, one gets totally different scenarios for DSs when the linear potential is applied. Indeed, in Fig. 3(b) we show the evolution of the DS in the nonlinear regime ($\gamma = 1$) with the linear potential parameter $\alpha = 0.02$. The initial profile of the DS is the one of the nonlinear DS plotted in Fig. 1(d). The input (red curve) and output (black curve) of this DS are plotted in Fig. 3(d). It is clearly demonstrated that, unlike JR states, DSs are very sensitive to the presence of linear potential. At the beginning, the beam (which initially is a DS) is bent downwards, like the Bloch oscillations; then, it strongly emits radiations, which totally destroy the structure of the DS. Later on, these radiations again gather together and form another beam with the output profile completely different from the input profile of the DS. Note that the linear potential parameter $\alpha = 0$ in Fig. 1, but $\alpha = 0.02$ in Fig. 3. Apart from that, all conditions and parameters for obtaining results in Fig. 3 are exactly the same as in Fig. 1.

So, we have demonstrated that the JR states are very robust under the influence of linear potential. The JR states are just localized at the interface between two BWAs and cannot be displaced or destroyed by the linear potential, unlike DSs. This amazing feature of JR states once more proves the robustness of JR states under strong disturbance and also has a root in the topological nature of JR states.

5. JACKIW–REBBI STATES AND DIRAC SOLITONS DYNAMICS WITH OBLIQUE INCIDENCE

All JR states and DSs analyzed above are normally launched into the system. In this section, we investigate the dynamics of JR states and DSs when they are launched obliquely into the system. Mathematically, this can be easily done if we multiply the initial JR states and DSs by an extra term in the form of $e^{in\varphi}$. Physically, this extra term represents the initial phase difference between fields at adjacent waveguides. In all cases shown above where beams are launched normally, this initial phase difference is just equal to zero, i.e., $\varphi = 0$. Now, in this section, as an example, we will set $\varphi = \pi/10$ for getting results in Fig. 4. All other conditions and parameters used in Fig. 4 are exactly the same as in Fig. 1.

In Fig. 4(a), we show the evolution of the JR state under the oblique incidence ($\varphi = \pi/10$). The initial profile of the JR state in Fig. 4(a) is also the one of the linear JR state plotted in Fig. 1(c). The input (red curve with round markers) and output (black curve) of this JR state are plotted in Fig. 4(c). It is quite unexpected that even the oblique incidence cannot displace the JR state from the interface between two BWAs. As clearly shown in Fig. 4(a), the JR state propagates just along the interface as if it was launched normally. As compared to the pure JR state shown in Figs. 1(a) and 1(c), the profile of the JR state in Figs. 4(a) and 4(c) is just slightly varied during propagation. This feature is also true if we use nonlinear JR states calculated in [33] instead of linear ones at the input.

On the contrary, we have a different scenario for the DS evolution under the oblique incidence ($\varphi = \pi/10$), as shown in Fig. 4(b). The initial profile of the DS is also the one of the nonlinear DS plotted in Fig. 1(d). The input (red curve) and output (black curve) of this DS are plotted in Fig. 4(d). It is clearly demonstrated that, unlike JR states, DSs are very sensitive to oblique incidence. As expected, the oblique incidence bends the DS, and as a result, the DS propagates under a certain angle inside the BWA. Although the DS emits some weak radiation during propagation in Fig. 4(b), the structure of the DS is also quite robust in this case.

So, we have demonstrated that the JR state is very robust under the oblique incidence in the sense that the JR state just propagates along the interface between two BWAs, whereas the

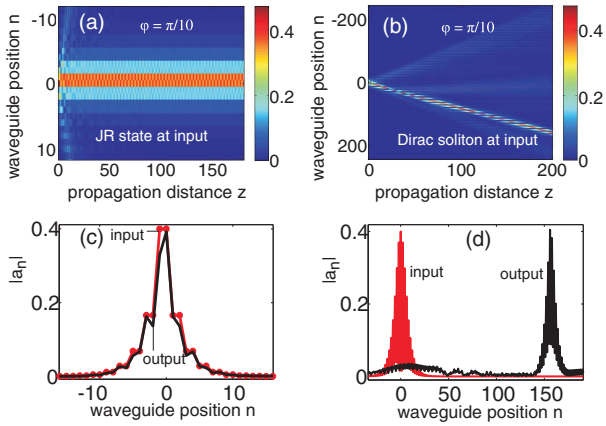

Fig. 4. (a), (b) Propagation of an initial JR state of the first type and an initial DS in BWAs, respectively, when they are both tilted at the input by imposing the initial phase difference $\varphi = \pi/10$ between two adjacent waveguides. (c) Input and output profiles of the JR state in (a). (d) Input and output profiles of the DS in (b). All other parameters (except for φ) are exactly the same as in Fig. 1.

DS can be easily shifted transversally as expected. This feature of JR states also has a root in their topological nature. Apart from this difference, the structures of both the JR state and the DS are rather robust in this case.

6. CONCLUSION

In conclusion, we demonstrate numerically that JR states formed at the interface between two BWAs are extremely robust under strong disturbance of various types such as the turning on/off of nonlinearity, the linear transverse potential, and the variation of the incidence angles. All of these types of strong disturbance cannot displace the JR states from the interface, neither can they destroy the JR states structure. This amazing feature of JR states is totally different from the DSs in BWAs or from other solitons in continuous media, which can be easily destroyed and/or displaced transversally under these strong disturbances. The robustness of JR states is due to the fact that they are topologically protected from many kinds of strong disturbance. This amazing feature of JR states in BWAs can have great potential for developing robust optical circuits.

Funding. Le Quy Don Technical University (19.ĐH.01).

REFERENCES

1. D. N. Christodoulides, F. Lederer, and Y. Silberberg, "Discretizing light behaviour in linear and nonlinear waveguide lattices," Nature **424**, 817–823 (2003).
2. A. L. Jones, "Coupling of optical fibers and scattering in fibers," J. Opt. Soc. Am. **55**, 261–271 (1965).
3. D. N. Christodoulides and R. I. Joseph, "Discrete self-focusing in nonlinear arrays of coupled waveguides," Opt. Lett. **13**, 794–796 (1988).
4. Y. S. Kivshar and G. P. Agrawal, *Optical Solitons: from Fiber to Photonic Crystals*, 5th ed. (Academic, 2003).
5. G. P. Agrawal, *Applications of Nonlinear Fiber Optics*, 2nd ed. (Academic, 2008).
6. T. X. Tran and F. Biancalana, "Diffractive resonant radiation emitted by spatial solitons in waveguide arrays," Phys. Rev. Lett. **110**, 113903 (2013).
7. T. X. Tran and F. Biancalana, "Mimicking the nonlinear dynamics of optical fibers with waveguide arrays: towards a spatiotemporal supercontinuum generation," Opt. Express **21**, 17539–17546 (2013).
8. T. X. Tran, D. C. Duong, and F. Biancalana, "Supercontinuum generation in both frequency and wave number domains in nonlinear waveguide arrays," Phys. Rev. A **89**, 013826 (2014).
9. U. Peschel, T. Pertsch, and F. Lederer, "Optical Bloch oscillations in waveguide arrays," Opt. Lett. **23**, 1701–1703 (1998).
10. T. Pertsch, P. Dannberg, W. Elflein, A. Bräuer, and F. Lederer, "Optical Bloch oscillations in temperature tuned waveguide arrays," Phys. Rev. Lett. **83**, 4752–4755 (1999).
11. G. Lenz, I. Talanina, and C. M. de Sterke, "Bloch oscillations in an array of curved optical waveguides," Phys. Rev. Lett. **83**, 963–966 (1999).
12. M. Ghulinyan, C. J. Oton, Z. Gaburro, L. Pavesi, C. Toninelli, and D. S. Wiersma, "Zener tunneling of light waves in an optical superlattice," Phys. Rev. Lett. **94**, 127401 (2005).
13. F. Dreisow, M. Heinrich, R. Keil, A. Tünnermann, S. Nolte, S. Longhi, and A. Szameit, "Classical simulation of relativistic Zitterbewegung in photonic lattices," Phys. Rev. Lett. **105**, 143902 (2010).
14. F. Dreisow, R. Keil, A. Tünnermann, S. Nolte, S. Longhi, and A. Szameit, "Klein tunneling of light in waveguide superlattices," Europhys. Lett. **97**, 10008 (2012).
15. T. X. Tran, S. Longhi, and F. Biancalana, "Optical analogue of relativistic Dirac solitons in binary waveguide arrays," Ann. Phys. **340**, 179–187 (2014).
16. A. A. Sukhorukov and Y. S. Kivshar, "Generation and stability of discrete gap solitons," Opt. Lett. **28**, 2345–2347 (2003).
17. M. Conforti, C. De Angelis, and T. R. Akylas, "Energy localization and transport in binary waveguide arrays," Phys. Rev. A **83**, 043822 (2011).
18. R. Morandotti, D. Mandelik, Y. Silberberg, J. S. Aitchison, M. Sorel, D. N. Christodoulides, A. A. Sukhorukov, and Y. S. Kivshar, "Observation of discrete gap solitons in binary waveguide arrays," Opt. Lett. **29**, 2890–2892 (2004).
19. M. Johansson, K. Kirr, A. S. Kovalev, and L. Kroon, "Gap and out-gap solitons in modulated systems of finite length: exact solutions in the slowly varying envelope limit," Phys. Scripta **83**, 065005 (2011).
20. A. Gorbach and M. Johansson, "Gap and out-gap breathers in a binary modulated discrete nonlinear Schrödinger model," Eur. Phys. J. D **29**, 77–93 (2004).
21. Y. S. Kivshar and N. Flytzanis, "Gap solitons in diatomic lattices," Phys. Rev. A **46**, 7972–7978 (1992).
22. T. X. Tran, X. N. Nguyen, and D. C. Duong, "Dirac soliton stability and interaction in binary waveguide arrays," J. Opt. Soc. Am. B **31**, 1132–1136 (2014).
23. T. X. Tran, X. N. Nguyen, and F. Biancalana, "Dirac solitons in square binary waveguide lattices," Phys. Rev. A **91**, 023814 (2015).
24. T. X. Tran and D. C. Duong, "Higher-order Dirac solitons in binary waveguide arrays," Ann. Phys. **361**, 501–508 (2015).
25. T. X. Tran and D. C. Duong, "Dirac light bullets in nonlinear binary waveguide arrays," Chaos **28**, 013112 (2018).
26. T. X. Tran, "Switching a Dirac soliton by a weak signal in binary waveguide arrays with varying propagation mismatch," J. Opt. Soc. Am. B **36**, 2001–2006 (2019).
27. D. D. Ivanenko, "Notes to the theory of interaction via particles," Sov. Phys. JETP **13**, 141–149 (1938).
28. W. Heisenberg, "Quantum theory of fields and elementary particles," Rev. Mod. Phys. **29**, 269–278 (1957).
29. M. Soler, "Classical, stable, nonlinear spinor field with positive rest energy," Phys. Rev. D **1**, 2766–2769 (1970).
30. J. Cuevas-Maraver, N. Boussaïd, A. Comech, R. Lan, P. G. Kevrekidis, and A. Saxena, "Solitary waves in the nonlinear Dirac equation," in *Nonlinear Systems* (Springer Nature, 2018), Vol. **1**.
31. T. X. Tran and F. Biancalana, "Linear and nonlinear photonic Jackiw–Rebbi states in interfaced binary waveguide arrays," Phys. Rev. A **96**, 013831 (2017).
32. R. Jackiw and C. Rebbi, "Solitons with fermion number 1/2," Phys. Rev. D **13**, 3398–3409 (1976).
33. T. X. Tran, H. M. Nguyen, and D. C. Duong, "Jackiw–Rebbi states in interfaced binary waveguide arrays with Kerr nonlinearity," Phys. Rev. A, submitted for publication.
34. T. X. Tran and F. Biancalana, "Interaction between Dirac solitons and Jackiw–Rebbi states in binary waveguide arrays," J. Lightwave Technol. **35**, 5092–5097 (2017).
35. R. B. Laughlin, "Nobel lecture: fractional quantization," Rev. Mod. Phys. **71**, 863–874 (1999).
36. M. Z. Hasan and C. L. Kane, "Topological insulator," Rev. Mod. Phys. **82**, 3045–3067 (2010).
37. M. C. Rechtsman, J. M. Zeuner, Y. Plotnik, Y. Lumer, D. Podolsky, F. Dreisow, S. Nolte, M. Segev, and A. Szameit, "Photonic Floquet topological insulators," Nature (London) **496**, 196–200 (2013).
38. N. N. Rosanov and T. X. Tran, "Interaction of dissipative Bragg solitons in active nonlinear fibers," Chaos **17**, 037114 (2007).
39. R. Morandotti, U. Peschel, J. S. Aitchison, H. S. Eisenberg, and Y. Silberberg, "Experimental observation of linear and nonlinear optical Bloch oscillations," Phys. Rev. Lett. **83**, 4756–4759 (1999).